# INVESTIGATION OF NEW CONCEPTS OF GROUND HEAT EXCHANGERS AND BUILDING INTEGRATED HEAT EXCHANGERS FOR PASSIVE HOUSES BY MEANS OF DYNAMIC BUILDING AND SYSTEM SIMULATION

Fabian Ochs[1], Georgios Dermentzis[1] and Wolfgang Feist[1,2]
[1]Institute of Construction and Material Science; Energy Efficient Buildings; University of Innsbruck, Innsbruck, Austria
[2]Passiv House Institute, Darmstadt, Germany

## ABSTRACT

Partial differential equations can be transformed in ordinary differential equations which can be solved with Simulink, using the Method of Lines. Thus, finite element models (here 2D based on Matlab PDETOOL) can be directly coupled to building and system simulation. This enables the solution of many complex building physics problems, such as solar heat pump systems and ground coupled heat pump systems with basket, trench or building integrated ground heat exchanger. For passive houses, a system with a ground coupled heat pumps with a building integrated ground heat exchanger is evaluated by means of simulation. The heat supply system, which includes a ground heat exchanger, a heat pump, a building and optionally solar thermal, is modeled using the simulation environment Matlab/Simulink and the Carnot Blockset. Based on the simulation, a heat pump calculation tool has been developed.

## INTRODUCTION

Passive houses show a well-balanced load duration curve, due to the very high level of thermal insulation and the resulting very low heating demand and load. The domestic hot water demand can be covered with a high fraction by solar energy. However, solar heating of passive houses is under most circumstances poorly effective as the heating demand is confined to few months in main winter. If, however, significant share, i.e. > 70 %, of the domestic hot water demand is covered by solar thermal, new configurations of ground heat exchangers may be feasible resulting in a significant cost reduction. However, careful planning is requried: over-dimensioning causes unnecessarily high costs, whereas an under-sized system can lead to low efficiency of the ground heat exchanger and heat pump and even to the failure of the system. In this paper it is discussed how different types of ground heat exchanger can be modeled with regard to accuracy and simulation performance.

## MODELING OF GROUND HEAT EXCHANGER

### General aspects

In contrast to borehole heat exchangers, horizontal ground heat exchangers are strongly influenced by weather conditions such as short-term and long-term variation of the ambient temperature, solar radiation and long-wave radiation as well as rain and snow (including thawing), due to the shallow depth (usually well below 5 m). In addition, freezing of the soil next to the pipes may play an important role.

In addition to the influence of ground water, diffusive moisture transport and influence of moisture-dependent thermal conductivity of the soil may be important. However, as shown by many authors (e.g. Rammin, 2007) heat conduction is the predominant effect.

Although, the modeling effort is significant, convergence is rather poor and usually the knowledge of the relevant parameters for the mechanisms mentioned above is limited. Thus, in many models only heat conduction in the ground is taken into account.

The influence of the long-wave and short-wave radiation can be taken into account by the use of solar air temperature (see Glück, 2009 and Ochs, 2011). If the ground heat exchanger is operated below the freezing temperature, freezing plays an important role (see corresponding section below).

### Coupling of the fluid and the solid domain

The ground heat exchanger can be considered as a semi-isothermal heat exchanger in simplified models. For the most common configurations, such as meander, harp and bifilar, 1D-models can be applied with little error. Assuming the surrounding soil of the pipe isothermal in pipe direction leads to negligible errors, even in case of trench or basket ground heat exchangers. Thus, the soil temperature is a function of the time and not of the position, $\vartheta_{HX} = f(t) \neq f(x)$ (see Figure 1). The outlet temperature $\vartheta_1''$ can be calculated as a function of the inlet temperature $\vartheta_1$' for steady state according to

$$\vartheta_1'' = \vartheta_1' - (\vartheta_1' - \vartheta_{HX}) \cdot \left(1 - e^{-\frac{UA}{\dot{C}}}\right) \quad (1)$$

and the heat transfer as follows

$$\dot{Q} = \dot{C} \cdot \left(\vartheta_1'' - \vartheta_1'\right) = UA \cdot \Delta\vartheta_{log} \quad (2)$$

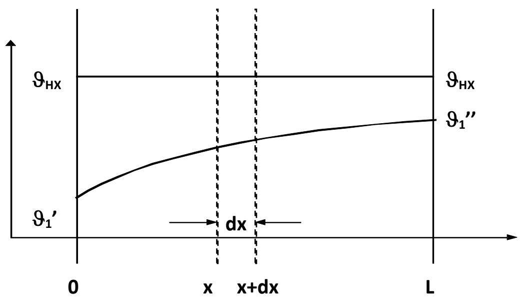


*Figure 1 Temperature profile of semi-isothermal heat exchanger with inlet temperature $\vartheta_1$', outlet temperature $\vartheta_1$'' and temperature of active layer $\vartheta_{HX}$; $\vartheta_{HX}$ can be a function of time ($\vartheta_{HX}=f(t)$)*

The heat flow is the product of the heat capacity flow $C = c \cdot \dot{m}$ and the difference of inlet and outlet temperatures $\vartheta_1$' and $\vartheta_1$'' and is equal to the product of the heat transfer capability UA and the logarithmic temperature difference:

$$\Delta\vartheta_{log} = \frac{(\vartheta_1' - \vartheta_{HX}) - (\vartheta_1'' - \vartheta_{HX})}{\ln\frac{(\vartheta_1' - \vartheta_{HX})}{(\vartheta_1'' - \vartheta_{HX})}} \quad (3)$$

The heat transfer capability UA is influenced by the geometry of the tubes (length, diameter, number and arrangement of the tubes), the fluid properties and the mass flow (laminar, turbulent). The logarithmic temperature difference is affected by the surrounding soil (temperature $\vartheta_{HX}$) and the operation of the ground heat exchanger.

The thermal resistance of the pipe corresponding to the internal pipe area $A = \pi \cdot d_i$ can be calculated by the U-value as follows:

$$U = \left(\frac{1}{h_i} + \frac{d_i}{2\lambda_p} \cdot \ln\frac{d_e}{d_i}\right)^{-1} \quad (4)$$

Discretization in the fluid direction is not required in most cases. In the relevant range of the number of transfer unit (NTU = C/UA < 2) of water or water/glycol based systems, one-node models can be used with a reasonable accuracy, see (Ochs, 2012).

The mean temperature can be approximated

$$\vartheta_m = \frac{\vartheta_1' + \vartheta_1''}{2} \quad (5)$$

and implemented in the Eq. (2):

$$\dot{Q} = UA \cdot (\vartheta_m - \vartheta_{hx}) \quad (6)$$

In case of one dimensional model (R-C), an effective heat transfer capability $UA_{eff}$ has to be found, depending on the distance of the pipes and the properties of the active ground layer (Ochs, 2011).

## Geometry

The majority of horizontal ground heat exchanger (e.g. meander, spiral, capillary type ground heat exchanger) can be modelled with a small error by an one dimensional R-C model (Figure 2, right). However, the performance of ground heat exchangers with a more complex geometry such as trench or basket collectors and construction integrated systems (Figure 2, left) can hardly be predicted with 1D-models. In case of symmetries the model can be simplified so that 2D models will serve in the majority of cases.

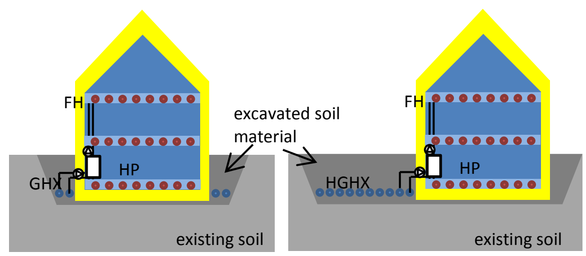


*Figure 2 Scheme of ground heat exchanger mounted in the surrounding excavation of the building (left) and horizontal ground heat exchanger (right)*

For complex geometries usually the Finite Element Method (FEM) is chosen. Matlab provides functions and interactive tools, such as the PDETOOL, to solve these problems.

## PDE, Method of Lines

Parabolic PDEs can be solved with the PDETOOL using the form

$$d \cdot u' - div(c \cdot grad(u)) + a \cdot u = f \quad (7)$$

where the coefficients d, c and f are a function of the position x and time t and are independent from the variable u. Applied to heat transfer, Eq. (7) forms to:

$$\rho \cdot c_p \cdot \frac{\partial\vartheta}{\partial t} - div(\lambda \cdot grad(\vartheta)) + a \cdot \vartheta = \dot{q} \quad (8)$$

The temperature $\vartheta$ is a function of the position x, the time t and the heat source $\dot{q}$. The thermal conductivity $\lambda$, and the volumetric capacity $\rho \cdot c_p$ can be functions of space and time but not of temperature.

Using the Method of Lines, (see Ruffaldi and Prüfert) the PDE can be transformed in an ODE that can be solved using Simulink.

$$\frac{d}{dt}U = M^{-1}\left(F + G + R + KU + QU + HU\right) \tag{9}$$

Here, U is the dependent variable, K is the stiffness matrix, M is the mass matrix, F is the right side vector, Q is for the system matrix and G is the u related term. H and R are zero in case of Neumann BC and nonzero in case of Dirichlet BC. The process is schematically shown in Figure 3.

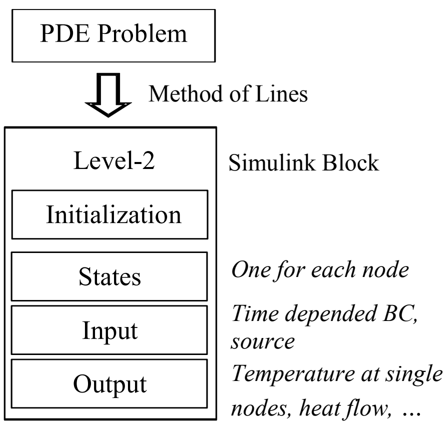


*Figure 3 Schematic approach of solving PDEs within the Simulink environment*

Simulink solves ODEs. These ODEs are generated from PDEs with the Method of Lines. The PDE parameters are updated with time, the integration is performed by Simulink. A Level-2 S-function can be used. In the Block *Initialization* the States of the PDE are initialized (one state for each node). The update of the derivatives (Method of Lines) is performed in the *Derivatives* Block. The *Outputs* are e.g. the temperatures at the nodes, the fluid outlet temperature (with given inlet temperature and mass flow) or the heat flow.

Using the method of lines, the thermal conductivity λ, and the volumetric capacity ($\rho c_p$) can be functions of space, time and temperature.

### Example 1

The mesh of a simplified ground heat exchanger model shown schematically in Figure 4 (corresponding to a ground heat exchanger mounted in the surrounding excavation of the building, see Figure 2, left).

The corresponding temperature profile is presented in Figure 5. The surrounding area of the tubes is cooled due to the heat extraction. In this example, the heat transfer from the building to the ground is neglected.

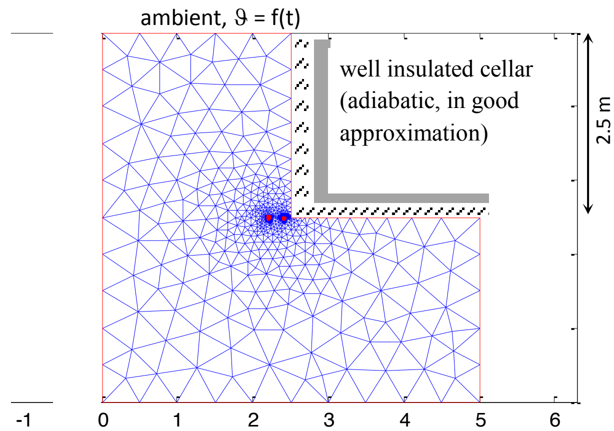


*Figure 4 Corresponding FE mesh for a ground heat exchanger mounted in the surrounding excavation of the building, coordinates x,z / [m]*

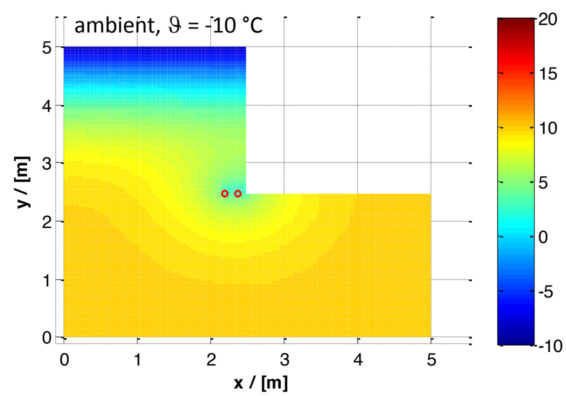


*Figure 5 Temperature distribution in °C for a ground heat exchanger mounted in the surrounding excavation of the building, arbitrary point of time, $\vartheta_{brine}$ = 0°C*

### Example 2

With a radial symmetric formulation of the PDE, a basket ground heat exchanger can be modeled in a similar way (Figure 6). The heat transfer equation is formulated to:

$$r\rho c_p \frac{\partial \vartheta}{\partial t} - \frac{\partial}{\partial r}\left( r\lambda \frac{\partial}{\partial r}\vartheta \right) - \frac{\partial}{\partial z}\left( \lambda \frac{\partial}{\partial z}\vartheta \right) = \dot{q}r \tag{10}$$

with radius r and depth z. The reduction of the extraction energy and power of neighboring baskets might be considered by reduced extension of the domain (or distance of the radial boundary, respectively). However, the reduction is overestimated if a neighboring basket is located only on one two or three sides.

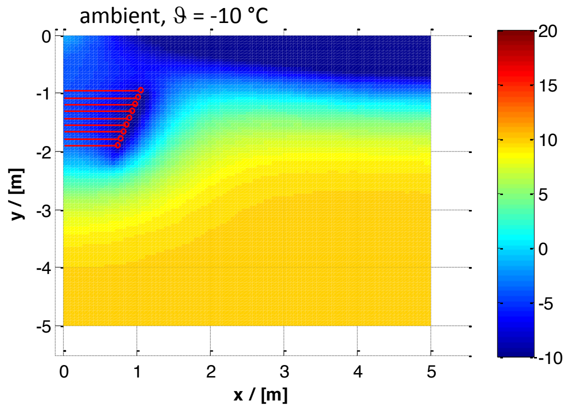


*Figure 6 Temperature distribution in °C for a basket type ground heat exchanger, arbitrary point of time, $\vartheta_{brine} = 0°C$*

**Example 3**

For the previous example of the ground heat exchanger mounted in the surroundings of the building (example 1), the temperature development of the brine (arithmetic mean between the inlet and outlet temperature) is presented in Figure 7 for two cases (1 loop and 2 loops). A single family house in passive house standard (heating area 140 $m^2$, heating demand 15 kWh/($m^2$ a), heating load 10 W/$m^2$, see Fig 7, bottom) with a heat pump (COP = 3) is the load for this study. The length of the ground heat exchanger is 44 m. The ambient temperature (e) is approximated by a sine function (annual mean temperature 10 °C, amplitude 10 K). Here, domestic hot water demand is not considered.

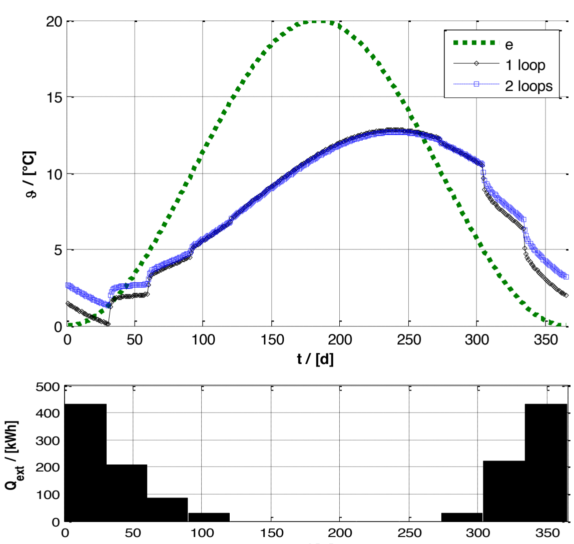


*Figure 7 (top) Development of brine temperature for the ground heat exchanger (example 1) with a typical heating load profile of a single family passive house (bottom) for the cases of 1 loop and 2 parallel loops;*

In this simple example, the heating period is from October to March. In summer the brine temperature represents the ground temperature, which is regenerating in this time and reaches approximately 13 °C before the start of heating period. The brine temperature in Figure 7 remains above the freezing point except from a short period in January. A safe operation above the freezing point is ensured using a second pipe loop. Then the brine temperature remains always above 2 °C.

A parametric study with respect to ground properties ($\lambda_{ground}$) and number of loops (1 or 2 ground heat exchanger loops) is summarized in table 1. The SFH 15 reference building with floor heating (as described in IEA SHC Task 44 with climate of Strasburg, but heat recovery of $\eta_{HRC} = 0.85$) is simulated exemplarily. A brine sourced heat pump (with COP (0/35) = 4.1) is directly connected to the ground heat exchanger and the floor heating system.

In case of 2 loops with normal ground thermal conductivity ($\lambda_{ground} = 2$ W/(m K)), reasonable performance of the heat pump can be recognized. In case of good properties of the ground ($\lambda_{ground} = 3$ W/(m K)), a system with 1 loop would be possible. For poor ground thermal conductivity ($\lambda_{ground} = 1$ W/(m K)), a backup heater would be required even in case of two loops. However, the performance is still reasonable.

*Table 1 Parametric study for ghx mounted in the surroundings of the building (example 1)*

| $\lambda_{ground}$ / [W/(m K)] | 1 | | 2 | | 3 | |
|---|---|---|---|---|---|---|
| No. loops | 1 | 2 | 1 | 2 | 1 | 2 |
| SPF / [-] | 3.93 | 4.34 | 4.38 | 4.75 | 4.74 | 4.88 |
| $W_{el}$ / [kWh] | 506 | 458 | 454 | 419 | 420 | 408 |
| $\vartheta_{sink}$ / [°C] | 31.2 | 32.1 | 32.4 | 32.8 | 32.8 | 33.1 |
| bivalent | x | x | x | | | |

**Freezing**

Ground heat exchangers are subject to freezing when installed in shallow depth and/or operated below 0°C (which is commonly the case with heat pumps). This effect can have significant influence on the brine temperatures and thus on the performance of the heat pump, depending on the soil and the share of soil moisture. Freezing has to be avoided in case of building integrated ground heat exchangers for static reasons.

Due to the latent heat of melting, the soil temperature remains at (or in the range of) 0°C until all moisture is frozen. Hence, a model which does not account for freezing would predict brine temperatures that are too low with corresponding lower performance of the heat pump. However, for obvious reasons the effect is only significant for moist soils.

Two methods to model freezing can be found in the literature: The Enthalphy method and the Heat Capacity method.

### Heat Capacity Method

The heat capacity method is applied here, as with a narrow temperature range (e.g. 2 K) it is more precise (see e.g. Lamberg et al. for further details). Based on a suggestion in (Comsol 2008) the material properties with the freezing effect are plotted in Figure 8. The fraction of frozen water (Θ) is modeled with a smoothed Heaviside function. The thermal conductivity (λ) and the density (ρ) change at phase transition (0 °C). The latent heat of fusion ($h_{sl}$) is considered using an apparent heat capacity, as shown in Figure 8. The apparent heat capacity accounts for the latent heat of fusion according to

$$c_p = \sum \Theta_i \rho_i \left(c_{p,i} + h_{sl} \cdot D\right) \qquad (11)$$

The pulse D is the derivative of the fraction of frozen water (Θ) with respect to temperature. In order to ensure energy conservation, it must apply that

$$\int_0^\infty \rho D h_{sl} dT = \rho \cdot h_{sl} \qquad (12)$$

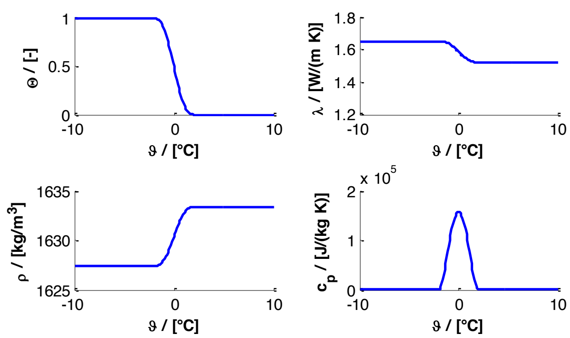


*Figure 8 Material properties as a function of temperature with phase transition at 0 °C with a pulse width of (here) ΔT = 1 K*

### Example 4

For an example of a meander and a capillary type ground heat exchanger the influence of freezing is investigated. Ground properties are listed in Table 2. See Table 3 for the dimensions and the parameters of the ground heat exchangers.

The course of the fluid temperature is plotted in Figure 9. For the capillary type ground heat exchanger without freezing, the mean brine temperature is about 1 K lower (-0.38 °C instead of 0.57 °C) and the minimum brine temperature is about 4 K lower (-7.65 °C instead of -3.5 °C).

The effect is similar for the meander but at a lower temperature level. The influence on the fluid temperature is in a similar range if the calculations are performed with ground type II instead of ground type I (mean: 2.04°C, min: -4.57 °C). The knowledge of the soil properties is of major importance.

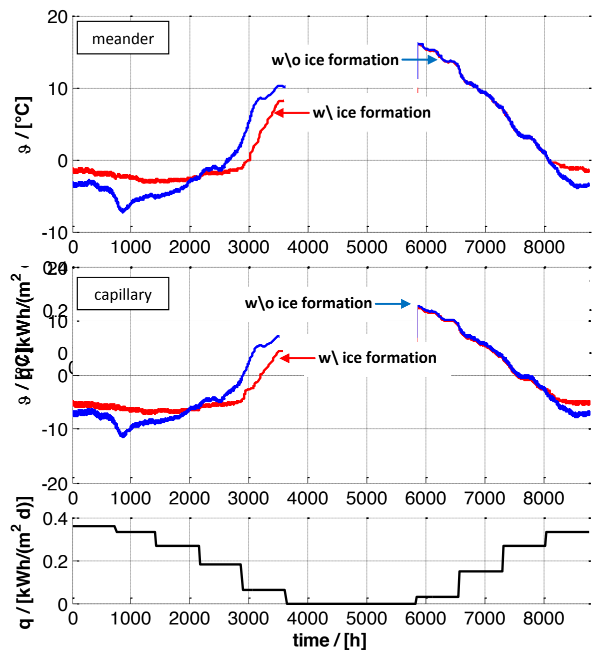


*Figure 9 Development of mean brine temperature with and without icing for meander (top) and capillary type (middle) ground heat exchanger for extracted power profile (bottom), max. extraction power $\dot{q}_c$ = 30 W/m², volume flow $\dot{V}$ = 3500 l/h (25 % Glycol), extraction energy $q_c$ = 60.84 kWh/(m² a), operation time $t_{op}$ = 2028 h*

*Table 2 Ground properties (acc. to Glück, 2009)*

| GROUND | TYP I SAND WITH CLAY 10 VOL% WATER CONTENT | | TYP II ROCK WITHOUT WATER |
|---|---|---|---|
| Phase | liquid | solid | - |
| Density ρ / [kg/m³] | 1630 | 1630 | 2400 |
| Heat conductivity λ / [W/(m K)] | 1.5 | 1.66 | 2.6 |
| Heat capacity $c_p$ / [J/(kg K)] | 1046 | 917 | 900 |
| Heat of fusion $h_{sl}$ / [kJ/kg] | 20.5 | | 0 |

*Table 3 Properties of meander and a capillary type ground heat exchanger*

| | MEANDER | CAPILLARY |
|---|---|---|
| |  | 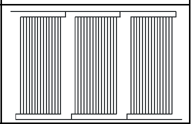 |
| Diameter $d_e$ /[mm] | 32 | 4.3 |
| Pipe thickness s/[mm] | 2.9 | 0.8 |
| Distance D/[mm] | 500 | 20 |
| Area A/[m²] | 100 | 100 |
| Length (straight) L/[m] | 8 | 5 |
| Number(parallel) $n_{par}$ /[-] | 25 | 1000 |
| Velocity w/[m/s ] | 0.9 | 0.17 |

### Validation

The results of the simulation models have been compared against other programs such as from Glück, 2009. Validation of a model of a vertical ground heat exchanger positioned below the building against measured data is shown in Ochs, 2011 and Ochs, 2012. Validation of a 1D model including freezing against measured data of a basket type ground heat exchanger from (Lose et al, 2013) is shown in Fig. 10:

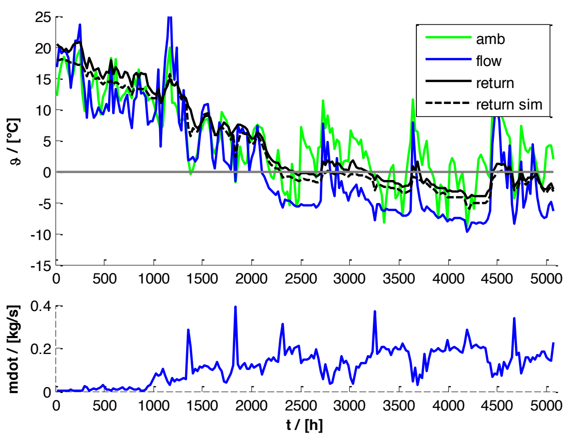


*Figure 10 Measured return temperature for a basket type ghx in comparison with simulated data with 1D ghx model including freezing*

Results are very promising. Further validation of the basket and trench type ground heat exchangers is part of future work.

## HEAT PUMP CALCULATION TOOL

A new calculation tool that allows the prediction of the annual electrical energy consumption and the seasonal performance factor (SPF) of heat pumps has been developed.

This new algorithm is based on the algorithm of the 'Compact' sheet (Pfluger, 2007) for compact units (heat pump and ventilation with heat recovery in one device), which is already available in Passive House Planning Package (PHPP). With the new heat pump tool higher accuracy can be achieved and the flexibility is improved:

- Several heat pump sources, such as ambient air, ground water, vertical or horizontal ground heat exchanger (GHX) can be chosen (air, water, brine).
- The heat pump can cover either the heating demand or the domestic hot water (DHW) demand or both.
- Several sink options and heating distribution systems are available, such as radiators, floor heating and air heating.
- There is the possibility of using two heat pumps in one building: One for covering heating demand and the other for domestic hot water.
- Two control strategies are available: The first is the common 'on/off' and the second the 'ideal' control system. The additional consideration of the 'ideal' control strategy gives the opportunity to predict the minimum possible electrical energy demand.
- There are a variety of storage options, e.g. same store for heating and DHW demand or two stores or heating distribution system without storage. Furthermore, there is an option concerning the location of the store (inside/outside of thermal envelope); store losses are gains in the heating period in case the store is inside.
- The contribution of solar thermal combined with a heat pump, is improved: solar thermal for DHW or heating and DHW.

### Method

As shown in Figure 10, the algorithm is based on the bin method. In case of air-sourced heat pumps 11 bins (10 for the heating period and 1 for the non-heating period) and in case of ground source heat pumps 4 bins (3 for the heating period and 1 for the non-heating period) are implemented.

The heating capacity of the heat pump and the heating load of the building are assumed to be linear. If the two lines intercept, the created triangle corresponds to the direct electricity ($W_{dir}$) and the system is called bivalent. Otherwise the system is monovalent and there is no need for direct electricity.

The heat supplied by the heat pump ($Q_{hp}$) in each bin is the area of bin. The COP of the heat pump is calculated also for each bin. The electrical energy consumption of the system is:

$$W_{el} = \sum \frac{Q_{hp}(bin)}{COP(bin)} + W_{dir} \qquad (13)$$

Solar thermal is implemented for DHW or heating and DHW, respectively. In case of heating, the solar fraction is implemented in the calculation of the duration of the heating period. Thus, the higher the ambient daily temperature in heating period, the more demand is covered by solar. In case of DHW, the energy which is covered by solar is divided in heating (winter) and non-heating (summer) period. The energy which is supplied by the heat pump ($Q_{hp}$) in the non-heating period is the DHW demand minus the demand which is covered by solar. In case of heating period, the demand covered by solar corresponds to a triangle or a trapeze, which is created by the line from points (1) and (2) in Figure 11. Therefore, the supplied energy by the heat pump ($Q_{hp}$) in each bin is the subtraction of the DHW demand and the demand covered by solar.

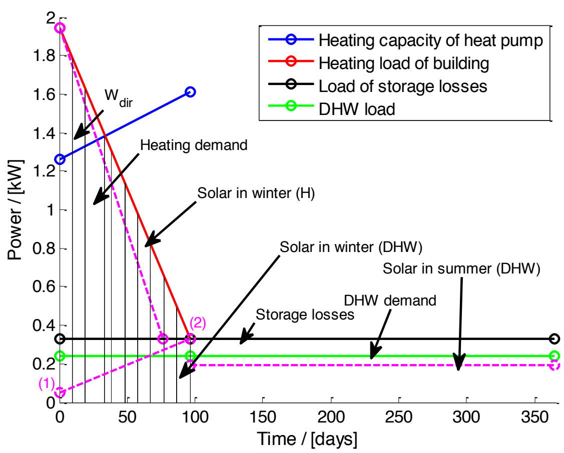


*Figure 11 Annual energy demand for air-sourced heat pump; example of a single family house in Passive House standard in Hamburg*

### Validation

Validation of the new heat pump calculation tool is performed by means of comparison with dynamic simulation in the Matlab/Simulink environment using models from the Carnot Blockset. The results of the calculation for the air-sourced heat pumps and ground sourced heat pumps with ground water or vertical ground heat exchanger show good agreement with the simulation results. Further validation will be performed.

## CONCLUSION

Ground sourced heat pumps have less operations costs than ambient or exhaust air heat pumps. However, the investment costs are higher. Thus, they are hardly economic in case of low energy demands such as in case of passive houses.

Due to the low energy demand and in particular due to the very low heat load of passive houses, new and more economic ground heat exchanger concepts can be developed. This applies in particular, if a significant share of the domestic hot water is covered by solar thermal.

Various types of ground heat exchanger are available such as horizontal, trench, basket and building integrated ones. Detailed planning of such systems by simulation is recommended as over-dimensioned systems are not economic and under-dimensioned systems have low efficiency and - in the worst case - can lead to total failure.

In order to simulate such heat pump systems, both short term (solar injection, freezing) and long term (cooling of the ground) effects should be included. Therefore, a fast and yet accurate enough simulation model of a building and a heat distribution and generation system is required.

This paper presents how a FE model can be integrated into dynamic building and systems simulation in Matlab/Simulink (using the Carnot Blockset) based on the method of lines. Different types of ground heat exchangers can be easily implemented in such a model. This gives the opportunity to simulate ground sourced heat pumps with high accuracy. An addressed future work may be the validation and the improvement of simulation performance.

Furthermore, a new flexible heat pump calculation tool has been developed and cross-validated, using the presented simulation models, accounting for different sources and sinks contribution of solar thermal.

## NOMENCLATURE

Latin

$A$ = area
$c_p$ = specific heat capacity
$D$ = pulse
$D$ = distance
$d$ = diameter
$F$ = right side vector
$f$ = flow term
$H$ = vector
$H$ = space heating in Figure 10
$h$ = heat transfer coefficient
$h_{sl}$ = heat of fusion
$i$ = run index
$K$ = stiffness matrix
$L$ = length
$M$ = mass matrix
$n$ = number
$Q$ = system matrix
$\dot{q}$ = heat flux
$R$ = vector
r = radius

*s* = source term
*s* = wall thickness
*T* = temperature
*U* = overall heat transfer coefficient
*U* = dependent variable
*u* = dependent variable
$W_{el(dir}$ =electrical energy/direct electric energy
*w* = velocity

Greek
ϑ = temperature
λ = thermal conductivity
ρ = density
θ = volume ratio

Abbreviations
*BC* = boundary conditions
*COP* = coefficient of performance
*DHW* = domestic hot water
*FEM* = finite element method
*FD* = finite difference
*FH* = floor heating
*GHX* = ground heat exchanger
*HP* = heat pump
*HX* = heat exchanger
*NTU* = number of transfer units
*ODE* = ordinary differential equation
*PDE* = partial differential equation
*PHPP* = Passive House Planning Package
*R-C* = resistance-capacitance

## ACKNOWLEDGEMENT

These results are part of the research and simulation work of the European project iNSPiRe funded under the 7th Framework Program (Proposal number: 314461, title: Development of Systematic Packages for Deep Energy Renovation of Residential and Tertiary Buildings including Envelope and Systems, duration: 01.10.2012 – 30.09.2016).

Thanks to ITW, University of Stuttgart, for sharing measured data of the basket type ghx for validation.

## REFERENCE

Dermentzis G., Ochs F., Feist W., Calculation of primary energy and seasonal performance factor of heat pump in a Passive House, PHI, internal document, Dec. 2012

Feist W., Arbeitskreis kostengünstige Passivhäuser, Protokollband Nr. 17 - Jahr 1999, Dimensionierung von Lüftungsanlagen in Passivhäusern, Darmstadt, 1999

Glück, B., Simulationsmodell "Erdwärmekollektor" zur wärmetechnischen Beurteilung von Wärmequellen, Wärmesenken und Wärme-/Kältespeichern, 2009

Ochs F., Peper S., Schnieders J., Pfluger R., Bianchi Janetti M., Feist W., Monitoring and Simulation of a Passive House with innovative Solar Heat Pump System, ISES Solar World Congress, Kassel, 2011

Loose A., Drück H., Feldtest von drei kombinierten Solarthermie-Wärmepumpenanlagen mit geothermischen Wärmequellen, 12. Internationales Anwenderforum Oberflächen-nahe Geothermie (OTTI), 2013, Deutschland

Ochs F., Feist W., Experimental Results and Simulation of Ground Heat Exchangers for a Solar and Heat Pump System for a Passive House, Proceedings of Innostock 2012, The 12th International Conference on Energy Storage, 2012, Lleida, Spain

Lamberg et al., Numerical and experimental investigation of melting and freezing processes in phase change material storage, I. J. of Thermal Sciences 43 (2004) 277–287.

Peper, S.; Schnieders, J.; Ochs, F., Feist, W.; Messtechnische Untersuchung und wissenschaftliche Auswertung zur saisonalen Wärmespeicherung über Sole-Register unter der Bodenplatte eines Passivhauses mit Dämmschürze,BBR, Darmstadt, 2010.

Pfluger R., Berechnung des primärenergiekennwertes und der Jahresarbeitszahl aus den Messwerten der Laborprüfung für die Zertifizierung von Passivhaus-Kompaktgeräten, PHI, State 19.1.2007, internal document, Jan. 2007

Prüfert U., PDEs lösen mit MATLAB, MATLAB PDE-Toolbox, Erweiterungen, Finite-Elemente auf Viereck-Gittern, TUB, 2010

Ruffaldi E., Elements of MATLAB and Simulink (2009), PERCRO, 2009

Ramming K.. Bewertung und Optimierung oberflächennaher Erdwärmekollektoren für verschiedene Lastfälle. PhD Thesis, TU Dresden, Dresden, Germany, 2007

Sparber W., Vajen K., Herkel S., Ruschemburg J., Thür A., Fedrizzi R., D'Antoni M., "Overview on solar thermal plus heat pump systems and review of monitoring results". ISES Solar World Congress, Kassel, Germany, 2011.

http://www.mathworks.com, 2011., CARNOT Blockset, V. R2009: Solar-Institut Jülich, 2009

http://www.comsol.com, 2011. Comsol, Model; Documentation, Phase Change, 2008

http://www.iea-shc.org/task44/, IEA SHC Task 44, HP Annex 38, 2012